

Received April 9, 2019, accepted May 3, 2019, date of publication May 10, 2019, date of current version May 31, 2019.

Digital Object Identifier 10.1109/ACCESS.2019.2916162

Hall Effect on Couple Stress 3D Nanofluid Flow Over an Exponentially Stretched Surface With Cattaneo Christov Heat Flux Model

ZAHIR SHAH¹, ABDULLAH DAWAR², EBRAHEEM O. ALZHRANI³,
POOM KUMAM^{4,5,6}, ABDUL JABBAR KHAN⁷, AND SAEED ISLAM¹

¹Department of Mathematics, Abdul Wali Khan University, Mardan 23200, Pakistan

²Department of Mathematics, Qurtuba University of Science and Information Technology, Peshawar 25000, Pakistan

³Department of Mathematics, Faculty of Science, King Abdulaziz University, Jeddah 21589, Saudi Arabia

⁴KMUTTFixed Point Research Laboratory, Room SCL 802 Fixed Point Laboratory, Science Laboratory Building, Department of Mathematics, Faculty of Science, King Mongkut's University of Technology Thonburi, Bangkok 10140, Thailand

⁵KMUTT-Fixed Point Theory and Applications Research Group, Theoretical and Computational Science Center, Science Laboratory Building, Faculty of Science, King Mongkut's University of Technology Thonburi, Bangkok 10140, Thailand

⁶Department of Medical Research, China Medical University Hospital, China Medical University, Taichung 40402, Taiwan

⁷University of Engineering and Technology Peshawar, Peshawar 25000, Pakistan

Corresponding author: Poom Kumam (poom.kum@kmutt.ac.th)

This research was funded by the Center of Excellence in Theoretical and Computational Science (TaCS-CoE), KMUTT.

ABSTRACT A recent challenging task in the field of nanotechnology is nanofluids, which are potential heat transfer fluids. Numerous researchers worked on nanofluid with different physical conditions. In this research work, we presented the three-dimensional flow of couple stress nanofluid with Hall current, viscous dissipation and Joule heating impacts past an exponentially stretching sheet. The Cattaneo–Christov heat flux model is implemented to examine the thermal relaxation properties. The modeled equations have been transformed to nonlinear ordinary differential equations with the help of correspondence transformations. The homotopy analysis method is used to solve the proposed model. The effect of dimensionless parameters, which are couple stress, Hartmann number, the ratio of rates, and Hall on velocity fields in x - and y -directions has been scrutinized. The rise in Hall parameter, Hartmann number, the ratio of rates parameter, and couple stress parameter are reducing the velocity function in the x -direction. The rise in Hall parameter, Hartmann number, and the ratio of rates parameter are improving the velocity function in the y -direction. The influence of Prandtl number, thermal relaxation time, and temperature exponent on temperature field are presented in this paper. The rise in thermal relaxation parameter, Prandtl number, and temperature exponent are reducing the temperature function. The influence of thermophoresis, the Schmidt number, and Brownian motion on concentration field are presented. The rise in thermophoresis parameter is increasing the concentration function while the rise in Brownian motion parameter and Schmidt number are reducing the concentration function. The impacts of implanted factors on skin friction, Nusselt number, and Sherwood number are accessible through tables. The determined result of skin friction is compared with the previous study.

INDEX TERMS Hall effect, MHD, nanofluid, couple stress fluid, thermal radiation, heat transfer, mass transfer.

NOMENCLATURE

A Temperature exponent
 B_0 Magnetic field strength (NmA^{-1})
 C Coefficient of concentration
 C_f Skin friction coefficient
 c_p Specific heat ($Jkg^{-1}K^{-1}$)
 D_B Brownian diffusion of nanofluids

D_T Thermophoretic diffusion of Nano fluids
 E Electric field (NC^{-1})
 f, g Dimensional velocity profiles
 J Current density (Am^{-2})
 K Couple stress parameter
 L Reference length (m)
 M Hartmann number
 m Hall parameter
 Nb Brownian motion

The associate editor coordinating the review of this manuscript and approving it for publication was Rahul A. Trivedi.

Nt	Thermophoretic parameter
Nu_x	Nusselt number
n_e	electrons density number(cm^{-3})
p_e	electronic pressure(Pa)
Pr	Prandtl number
q_r	Heat flux(Wm^{-2})
Re_x	Local Reynolds number
Sc	Schmidt number
Sh_x	Sherwood number
T	Fluid temperature(K)
U_0, V_0	Constants
u, v, w	Velocity components(ms^{-1})
x, y, z	Coordinate axis
$y_i(i = 1 - 10)$	Constants
<i>Greek Letters</i>	
ω_e	Frequency of electron(J)
τ_e	Collision time of electron
α	Ratio of rates parameter
Ω	Thermal relaxation time
γ	Biot number
θ	Dimensional heat profile
Φ	Dimensional concentration profile
ξ	Similarity variable
ν	Kinematic viscosity(m^2s^{-1})
λ_r	Relaxation time(s)
λ_r	Thermal conductivity(m^2s^{-1})
ρ	Fluid density(Kgm^{-3})
σ_{nf}	Electrical conductivity (Sm^{-1})

I. INTRODUCTION

The nanoparticles are particles between 1 and 100 nanometers in size with a surrounding interfacial layer. Nanofluids are castoff in microelectronics, hybrid powered machines, pharmaceutical procedures, fuel cells, and nanotechnologies' field. For the first time, Choi and Estman [1] presented the term nanoparticle immersed into a base fluid. Wang and Mujumdar [2] added the metallic and non-metallic particle into it and presented the heat transfer characteristics of the nanofluid. This study was trailed from the numerical study of Eastman *et al.* [3], [4]. They examined the heat transfer characteristics of nanofluid considering different nanoparticles as base fluid. Considering TiO_2 as base fluid, the thermal conductivity of nanofluid was examined by Murshed *et al.* [5]. In uniform heated tube Maïga *et al.* [6] examined the heat transfer in a nanofluid. They considered water- γAl_2O_3 and ethylene glycol- γAl_2O_3 nanofluids as based fluid. They claimed that under consideration of these nanofluids, the heat transfer is increased. They also originate that ethylene glycol- γAl_2O_3 nanofluid has well increment in heat transfer phenomena than the water- γAl_2O_3 nanofluid. Bianco *et al.* [7] numerically examined the water- γAl_2O_3 nanofluid flow in a flat tube. Tiwari and Das [8] introduced the single phase model, while Buongiorno [9] introduced the second phase model for nanofluids. Succeeding these models, copious investigators have functionalized in different

areas of attentiveness. Kasaieian *et al.* [10] scrutinized the heat transfer performance of nanofluid flow in a porous media.

The boundary value problem for impacts of Hall and ion-slip current and chemical reaction in micro-polar fluid flow has been examined by Motsa and Shateyi [11]. The peristaltic viscous fluid flow with convective boundary conditions in a rotating channel has been scrutinized by Hayat *et al.* [12]. Hayat and Nawaz [13] probed the impact of Hall and ion-slip on the second grade fluid flow. Hayat *et al.* [14] inspected the impact of Hall current and chemical reactions on peristaltic fluid flow. Hayat *et al.* [15] examined the impact of Hall and ion-slip on three-dimensional mixed convection flow of fluid. Hayat and Nawaz [16] scrutinized the impacts of Soret and Dufour on the second grade fluid flow subject to Hall and ion-slip current. Hayat *et al.* [17] deliberated the peristaltic nanofluid flow with joule heating, Hall and ion-slip current impacts. Nawaz *et al.* [18] examined the three-dimensional flow of nanofluid with Hall and ion-slip impacts. Recently, Nawaz *et al.* [19] examined the impacts of Hall and ion-slip on three-dimensional flow of micro-polar fluid. Hayat *et al.* [20] examined the impact of Hall current on couple stress fluid flow in an inclined symmetry channel.

Ramzan *et al.* [21] inspected the radiative magnetohydrodynamic (MHD) flow of nanofluid. Considering porous enclosure, Sheikholeslami and Shehzad [22] numerically examined the MHD flow of nanofluid. Besthapu *et al.* [23] examined the mixed convection flow of MHD nanofluid with the impact of viscous dissipation. Dawar *et al.* [24] scrutinized the flow of nonofluid over an unsteady oscillatory porous stretched sheet. Alharbi *et al.* [25] examined [24] with entropy generation considering the magnetic field impact. Shah *et al.* [26] examined the Darcy-Forchheimer nanofluid flow with inertial characteristics in a rotating frame. Khan *et al.* [27] scrutinized the MHD flow of Darcy-Forchheimer nanofluid with thermal radiation impact. Khan *et al.* [28] scrutinized the 2-D flow of nanofluid over a linear stretched surface. Dawar *et al.* [29] probed the MHD nanofluid flow considering entropy generation viscous dissipation. Sheikholeslami [30] numerically observed the free convective nanofluid in a porous enclosure under electric field impact. In another article, Sheikholeslami [31] investigated the flow of CuO- water nanofluid with the impacts of magnetic field and Brownian motion. Dawar *et al.* [32] analytically scrutinized the Darcy-Forchheimer flow of nanofluid over a stretched sheet with convective conditions. Ramzan *et al.* [33] scrutinized the 3-D MHD couple stress nanofluid flow on convective heat and zero mass flux conditions.

In 1822, Fourier [34] proposed a model for heat transmission in materials. In 1948, Cattaneo [35] further modified the Fourier law with thermal relaxation time. After then, Christov [36] has further amended the model [35] and is recognized as Cattaneo-Christov model for heat flux. Using the Cattaneo-Christov heat flux model, in a porous media, Straughan [37] deliberated the stability and wave motion. In another article, Straughan [38] examined the heat transfer

in nanofluid. Han *et al.* [39] inspected the heat transfer for viscoelastic fluids. Khan *et al.* [40] numerically investigated [39] over an exponentially stretched sheet. Hayat and Nadeem [41] examined the nanofluid flow with Cattaneo-Christov heat flux model and chemical processes over a stretching sheet. Tibullo and Zampoli [42] examined the model [36] for incompressible fluids. Ciarletta and Straughan [43] deliberated the stability and uniqueness of model [36]. Haddad [44] examined the thermal stability of the model [36] in porous media. Mustafa [45] used the model [36] for heat transfer and rotating flow of nanofluid. Hayat *et al.* [46] scrutinized the influence of the model [36] in the flow of fluids. Waqas *et al.* [47] deliberated the thermal conductivity of Burgers fluid using the model [36] for heat flux. Using model [36], Li *et al.* [48] examined the viscoelastic MHD fluid flow and heat transfer over a stretched sheet. Shah *et al.* [49] examined the MHD electrical ferrofluid nanofluid with model [36] over a stretching sheet. Hayat *et al.* [41] examined the 3-D nanofluid flow with model [36] over stretching surface. Muskat [50] scrutinized the homogeneous fluids flow in a porous media. Seddeek [51] deliberated the Darcy-Forchheimer flow of mixed convention fluid with thermophoresis and viscous dissipation impacts. Pal and Mondal [52] examined the Darcy-Forchhemier flow in a porous media. Sadiq and Mondal [53] deliberated the Darcy-Forchhemier flow of MHD Maxwell nanofluid with heated sheet. Gul [54] examined the scattering of thin layer over a nonlinear extending surface. Gul *et al.* [55] examined the thin film nanofluid flow on a rotating disk. Ali *et al.* [56] scrutinized the MHD flow thin film fluid with thermophoresis and variable fluid properties. Gohar *et al.* [57] examined the thin film flow single-walled and multi-walled carbon nanotubes over a nonlinear extending disc. Gul *et al.* [58] studied the entropy generation in a thin film flow over a stretching sheet. Khan *et al.* [59] examined the MHD thin film second grade fluid past a stretching sheet with thermophoresis and thermal radiation impacts. Gireesha *et al.* [60] examined the MHD mixed convection Casson nanofluid flow under the influences of ohmic heating and cross diffusion. Ganesh Kumar *et al.* [61] examined the Burgers nanofluid over a stretching sheet with non-uniform heat source/sink and nonlinear radiation impacts. Gireesha *et al.* [62] inspected the MHD nonfluid flow containing gyrotactic microorganism with chemical reaction. The other related studies can be seen in [63]–[69].

Keeping in observation the overhead literature review, we are able to study the 3-D flow of couple stress nanofluid with Hall current past an exponentially porous stretching sheet. It should be noted that this model is presented with joule heating and viscous dissipation influences. To study the relaxation properties, the Cattaneo-Christov heat flux model is employed. For the very first time, the impact of temperature exponent is examined in the literature.

II. PROBLEM FPRMULATION

Assume the 3-D flow of couple stress nanofluid past an exponentially porous stretching sheet with zero mass flux

and convective heat conditions. The stretched velocity along x -direction is considered as $u = U_w(x, y) = U_0 e^{(x+y/L)}$ whereas the velocity along y -direction is considered as $v = V_w(x, y) = V_0 e^{(x+y/L)}$ where (U_0, V_0) are constants. Uniform magnetic field impacts are considered in the nanofluid flow. The uniform magnetic field is applied along y -direction. The porous stretching surface is kept at constant temperature T_w and the ambient temperature T_∞ . Also C_w indicates the constant concentration and C_∞ indicates the ambient concentration.

Keeping in view the above assumption, the Ohm's law along with Hall current is of the form;

$$\mathbf{J} + \frac{\omega_e \tau_e}{B_0} \times (\mathbf{J} \times \mathbf{B}) = \sigma_{nf} \left(\mathbf{E} + \mathbf{V} \times \mathbf{B} + \frac{1}{en_e} P_e \right) \quad (1)$$

where $\mathbf{J} = (J_x, J_y, J_z)$ is the current density vector, \mathbf{B} is the magnetic induction vector applied in y -axis, \mathbf{E} is the electric field intensity vector, $\mathbf{V} = (u, v, w)$ is the velocity vector, σ is the effective electrical conductivity, ω_e is the frequency of electron, τ_e is the collision time of electron, e is the electron charge, n_e is the electron density number and p_e is the electronic pressure. Since no voltage is imposed on the fluid flow therefore, electric field becomes as $\mathbf{E} = 0$. So the components of the current density become

$$J_x = \frac{\sigma B_0}{(1+m^2)} (mu - v), \quad (2)$$

$$J_y = \frac{\sigma B_0}{(1+m^2)} (u - mv), \quad (3)$$

where $m = \omega_e \tau_e$ is Hall parameter.

The principal equations for the demonstrated problem are as [33], [41]:

$$\frac{\partial u}{\partial x} + \frac{\partial v}{\partial y} + \frac{\partial w}{\partial z} = 0, \quad (4)$$

$$u \frac{\partial u}{\partial x} + v \frac{\partial u}{\partial y} + w \frac{\partial u}{\partial z} = \nu \frac{\partial^2 u}{\partial z^2} - \nu' \frac{\partial^4 u}{\partial z^4} + \frac{\sigma B_0^2}{(1+m^2)\rho} (v - mu), \quad (5)$$

$$u \frac{\partial v}{\partial x} + v \frac{\partial v}{\partial y} + w \frac{\partial v}{\partial z} = \nu \frac{\partial^2 v}{\partial z^2} - \nu' \frac{\partial^4 v}{\partial z^4} - \frac{\sigma B_0^2}{(1+m^2)\rho} (mu - v), \quad (6)$$

$$\rho c_p \left(u \frac{\partial T}{\partial x} + v \frac{\partial T}{\partial y} + w \frac{\partial T}{\partial z} \right) = -\nabla \cdot \vec{q}, \quad (7)$$

$$u \frac{\partial C}{\partial x} + v \frac{\partial C}{\partial y} + w \frac{\partial C}{\partial z} = D_B \left(\frac{\partial^2 C}{\partial z^2} \right) + \frac{D_T}{T_\infty} \left(\frac{\partial^2 T}{\partial z^2} \right). \quad (8)$$

The heat flux \vec{q} satisfies

$$\vec{q} + \lambda_r \left(\frac{\partial \vec{q}}{\partial t} + \vec{V} \cdot \nabla \vec{q} - \vec{q} \cdot \nabla \vec{V} + (\nabla \cdot \vec{V}) \vec{q} \right) = -\lambda_c \nabla T, \quad (9)$$

where λ_r and λ_c signify the thermal relaxation time and thermal conductivity. Reducing equation (9) to Fourier's law

(i.e. taking $\lambda_r = 0$). Now, excluding \vec{q} from equations (4) and (6), the heat equation is reduced as:

$$\begin{aligned}
 u \frac{\partial T}{\partial x} + v \frac{\partial T}{\partial y} + w \frac{\partial T}{\partial z} &= \frac{\lambda_c}{\rho c_p} \left(\frac{\partial^2 T}{\partial z^2} \right) - \lambda_r \left[u^2 \frac{\partial^2 T}{\partial x^2} + v^2 \frac{\partial^2 T}{\partial y^2} \right. \\
 &+ w^2 \frac{\partial^2 T}{\partial z^2} + 2uv \frac{\partial^2 T}{\partial x \partial y} + 2vw \frac{\partial^2 T}{\partial y \partial z} \\
 &+ 2uw \frac{\partial^2 T}{\partial x \partial z} + \left(u \frac{\partial u}{\partial x} + v \frac{\partial u}{\partial y} + w \frac{\partial u}{\partial z} \right) \frac{\partial T}{\partial x} \\
 &+ \left(u \frac{\partial v}{\partial x} + v \frac{\partial v}{\partial y} + w \frac{\partial v}{\partial z} \right) \frac{\partial T}{\partial y} \\
 &+ \left. \left(u \frac{\partial w}{\partial x} + v \frac{\partial w}{\partial y} + w \frac{\partial w}{\partial z} \right) \frac{\partial T}{\partial z} \right], \quad (10)
 \end{aligned}$$

with boundary conditions

$$\begin{aligned}
 u &= U_w(x, y) = U_0 e^{(x+y)/L}, v = V_w(x, y) = V_0 e^{(x+y)/L}, \\
 w &= 0, k \frac{\partial T}{\partial z} = -h_f (T_w - T), \\
 D_B \frac{\partial C}{\partial z} + \frac{D_T}{T_\infty} \frac{\partial T}{\partial z} &= 0, \text{ at } z = 0, \\
 u \rightarrow 0, v \rightarrow 0, C \rightarrow C_\infty, T \rightarrow T_\infty \text{ as } z \rightarrow \infty. \quad (11)
 \end{aligned}$$

In the exceeding equations, u, v, w are the velocity components in their corresponding directions, kinematic viscosity (ν), thermal conductivity (k), couple stress viscosity ($\nu' = n/p$) where n is the viscosity parameter, heat transfer coefficient (h_f), electric charge density (σ), density (ρ), temperature exponent (A), specific heat (c_p), coefficient of Brownian diffusion (D_B), is the reference length (L), thermophoretic diffusion coefficient (D_T).

Using the following transformations

$$\begin{aligned}
 u &= U_0 e^{(x+y)/L} f'(\xi), v = U_0 e^{(x+y)/L} g'(\xi), \\
 w &= -\sqrt{\frac{\nu U_0}{2L}} e^{(x+y)/2L} \left\{ \begin{aligned} f(\xi) + \xi f'(\xi) \\ + g(\xi) + \xi g'(\xi) \end{aligned} \right\}, \\
 T_w &= T_\infty + T_0 e^{A(x+y)/2L} \theta(\xi), \\
 C_w &= C_\infty + C_0 e^{A(x+y)/2L} \Phi(\xi), \\
 \xi &= \sqrt{\frac{U_0}{2\nu L}} e^{(x+y)/2L} z. \quad (12)
 \end{aligned}$$

Equation (4) is gratified inexorably, and equations (5)-(10) yield

$$\begin{aligned}
 \frac{d^3 f}{d\xi^3} - 2 \left\{ \frac{df}{d\xi} + \frac{dg}{d\xi} \right\} \frac{df}{d\xi} + \{f + g\} \frac{d^2 f}{d\xi^2} \\
 - K \frac{d^5 f}{d\xi^5} + \frac{M^2}{1 + m^2} \left\{ \frac{dg}{d\xi} - m \frac{df}{d\xi} \right\} = 0, \quad (13)
 \end{aligned}$$

$$\begin{aligned}
 \frac{d^3 g}{d\xi^3} - 2 \left\{ \frac{df}{d\xi} + \frac{dg}{d\xi} \right\} \frac{dg}{d\xi} + \{f + g\} \frac{d^2 g}{d\xi^2} \\
 - K \frac{d^5 g}{d\xi^5} - \frac{M^2}{1 + m^2} \left\{ m \frac{df}{d\xi} - \frac{dg}{d\xi} \right\} = 0, \quad (14)
 \end{aligned}$$

$$\begin{aligned}
 \frac{1}{Pr} \frac{d^2 \theta}{d\xi^2} - A \left\{ \frac{df}{d\xi} + \frac{dg}{d\xi} \right\} \theta + \{f + g\} \frac{d\theta}{d\xi} \\
 + \frac{\Omega}{2} \left[\left\{ \xi \left\{ \frac{df}{d\xi} + \frac{dg}{d\xi} \right\} + (1 + 2A) \{f + g\} \right\} \right]
 \end{aligned}$$

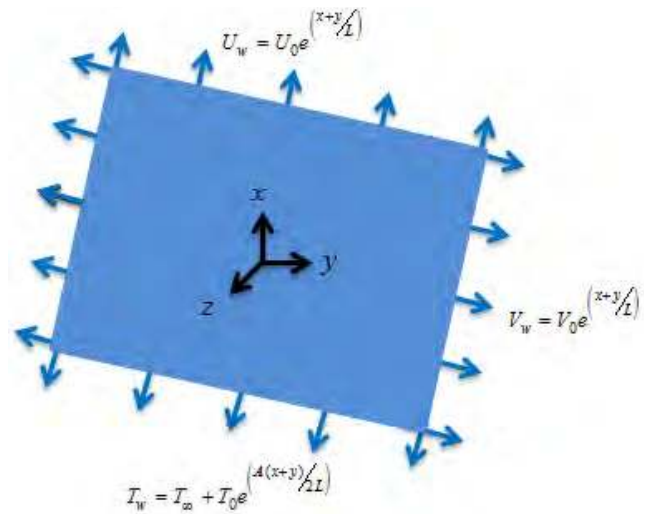


FIGURE 1. Geometrical illustration of the fluid flow [33].

$$\begin{aligned}
 \times \left\{ \frac{df}{d\xi} + \frac{dg}{d\xi} \right\} \frac{d\theta}{d\xi} - A \left\{ (A + 2) \left\{ \frac{df}{d\xi} + \frac{dg}{d\xi} \right\}^2 - \right. \\
 \left. \{f + g\} \left\{ \frac{d^2 f}{d\xi^2} + \frac{d^2 g}{d\xi^2} \right\} \right\} \theta \\
 - \{f + g\}^2 \frac{d^2 \theta}{d\xi^2} = 0, \quad (15)
 \end{aligned}$$

$$\begin{aligned}
 \frac{d^2 \Phi}{d\xi^2} - ScA \left\{ \frac{df}{d\xi} + \frac{dg}{d\xi} \right\} \Phi \\
 + Sc \{f + g\} \frac{d\Phi}{d\xi} + \frac{Nt}{Nb} \frac{d^2 \theta}{d\xi^2} = 0, \quad (16)
 \end{aligned}$$

which satisfy the following boundary conditions

$$\begin{aligned}
 f = 0, \frac{df}{d\xi} = 1, g = 0, \frac{dg}{d\xi} = \alpha, \frac{d\theta}{d\xi} \\
 = -\gamma (1 - \theta), Nb \frac{d\Phi}{d\xi} + Nt \frac{d\theta}{d\xi} = 0 \text{ at } \xi = 0, \\
 \frac{df}{d\xi} \rightarrow 0, \frac{dg}{d\xi} \rightarrow 0, \theta \rightarrow 0, \Phi \rightarrow 0 \text{ as } \xi \rightarrow \infty. \quad (17)
 \end{aligned}$$

In equations (12)-(16), $K = \frac{\nu'a}{\nu^2}$ represents the dimensionless couple stress parameter, $M^2 = \frac{2\sigma B_0^2 L}{\rho U_w}$ represents the Hartmann number, $\alpha = \frac{V_0}{U_0}$ represents the ratio of rates parameter, $Pr = \frac{\nu \rho c_p}{\lambda_c}$ represents the Prandtl number, $\Omega = \frac{\lambda_r U_w}{L}$ represents dimensionless thermal relaxation time, $\gamma = \frac{h}{k} \sqrt{\frac{2\nu L}{U_w}}$ indicates the Biot number, $Sc = \frac{\nu}{D_B}$ represents Schmidt number, $Nb = \frac{\tau D_B}{\nu} (C_w - C_\infty)$ represents the Brownian motion parameter and $Nt = \frac{\tau D_T (T_w - T_\infty)}{\nu T_\infty}$ represents thermophoresis parameter.

The equations of skin friction coefficients, local Nusselt number, and Sherwood number are:

$$\begin{aligned}
 C_{fx} \left(\frac{Re_x}{2} \right)^{1/2} &= e^{\left(\frac{3(x+y)}{2L} \right)} \frac{d^2 f(0)}{d\xi^2}, \\
 C_{fy} \left(\frac{Re_x}{2} \right)^{1/2} &= e^{\left(\frac{3(x+y)}{2L} \right)} \frac{d^2 g(0)}{d\xi^2},
 \end{aligned}$$

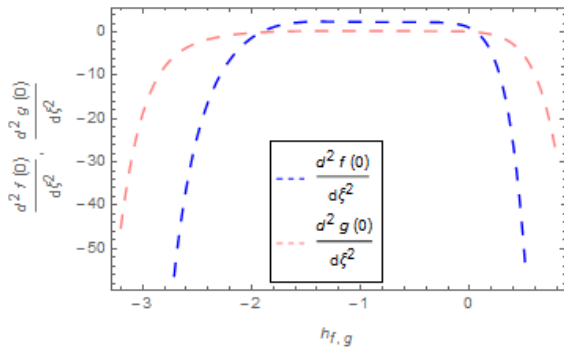


FIGURE 2. h -curves for velocities fields.

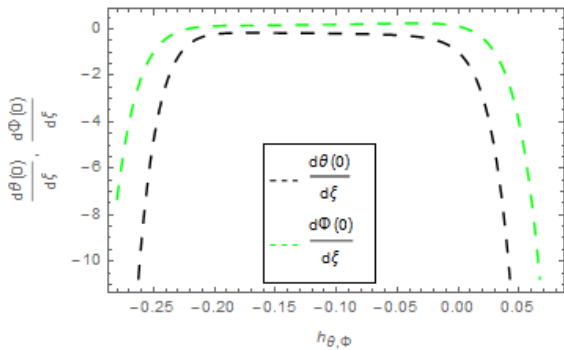


FIGURE 3. h -curves for temperature and concentration fields.

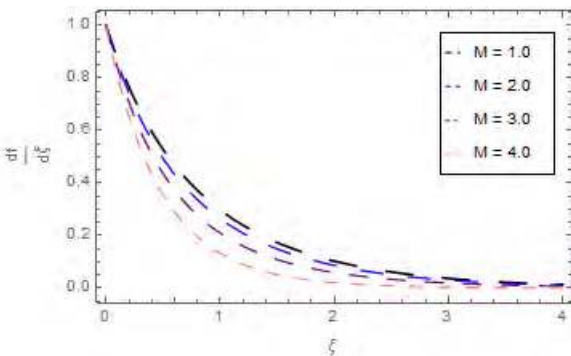


FIGURE 4. Impression of M on $\frac{df}{d\xi}$.

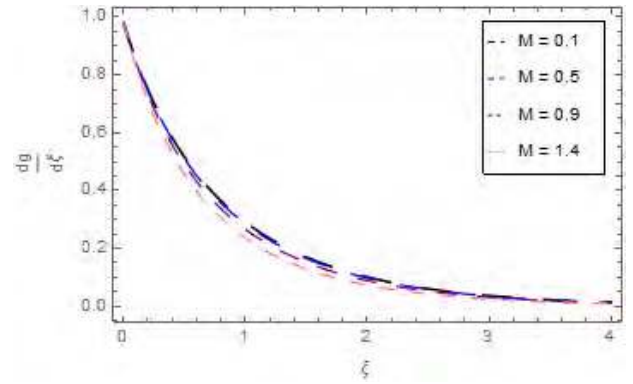


FIGURE 5. Impression of M on $\frac{dg}{d\xi}$.

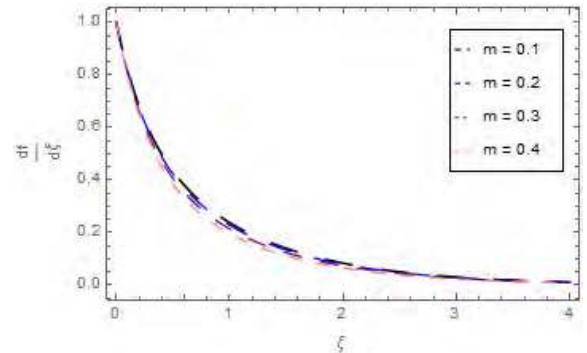


FIGURE 6. Impression of m on $\frac{df}{d\xi}$.

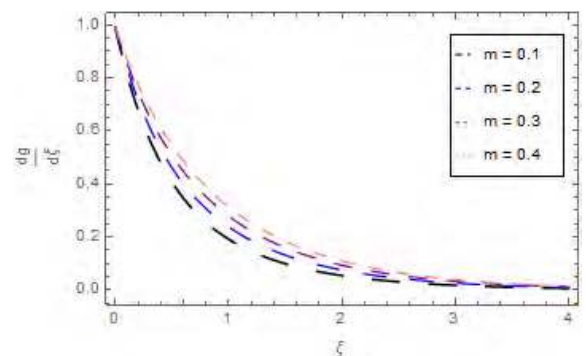


FIGURE 7. Impression of m on $\frac{dg}{d\xi}$.

$$\begin{aligned} \frac{L}{x} Nu_x \left(\frac{Re_x}{2} \right)^{1/2} &= -e^{(x+y)2L} \frac{d\theta(0)}{d\xi}, \\ \frac{L}{x} Sh_x \left(\frac{Re_x}{2} \right)^{1/2} &= -e^{(x+y)2L} \frac{d\Phi(0)}{d\xi}, \end{aligned} \quad (18)$$

where $Re_x = \frac{U_0 L}{\nu}$ is the Reynolds number.

III. SOLUTION BY HAM

In this section we used HAM to solve the equations (13)-(16) with boundary condition (17). The successive process is used to solve the equations by HAM.

The initial suppositions are chosen as:

$$\begin{aligned} f_0(\xi) &= 1 - e^{-\xi}, \quad g_0(\xi) = \alpha (1 - e^{-\xi}), \\ \theta_0(\xi) &= \left(\frac{\gamma}{1 + \gamma} \right) e^{-\xi}, \quad \Phi_0(\xi) = - \left(\frac{Nb}{Nt} \frac{\gamma}{1 + \gamma} \right) e^{-\xi}. \end{aligned} \quad (19)$$

The L_f, L_g, L_θ and L_Φ are picked as:

$$\begin{aligned} L_f(f) &= \frac{d^3 f}{d\xi^3} - \frac{df}{d\xi}, \quad L_g(g) = \frac{d^3 g}{d\xi^3} - \frac{dg}{d\xi}, \\ L_\theta(\theta) &= \frac{d^2 \theta}{d\xi^2} - \theta, \quad L_\Phi(\Phi) = \frac{d^2 \Phi}{d\xi^2} - \Phi, \end{aligned} \quad (20)$$

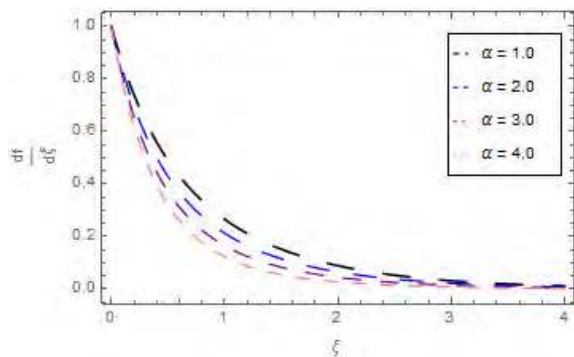


FIGURE 8. Impression of α on $\frac{df}{d\xi}$.

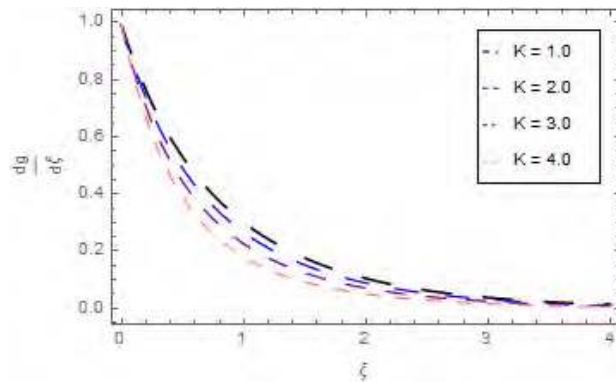


FIGURE 11. Impression of K on $\frac{dg}{d\xi}$.

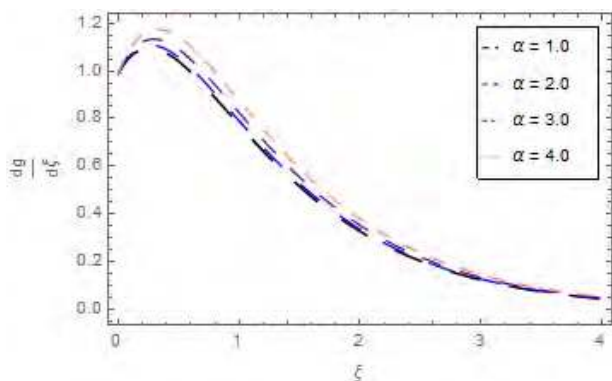


FIGURE 9. Impression of α on $\frac{dg}{d\xi}$.

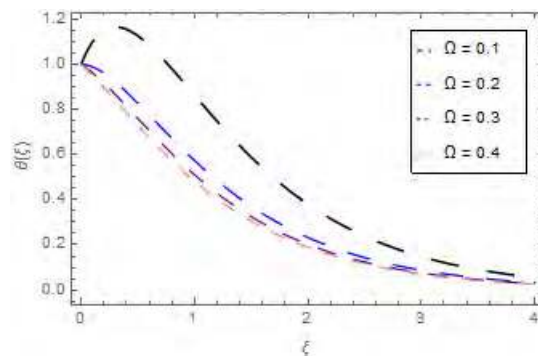


FIGURE 12. Impression of Ω on $\theta(\xi)$.

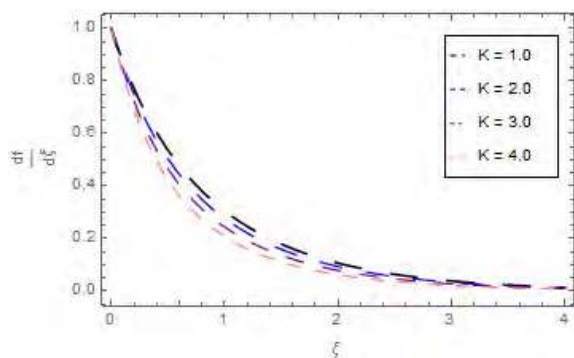


FIGURE 10. Impression of K on $\frac{df}{d\xi}$.

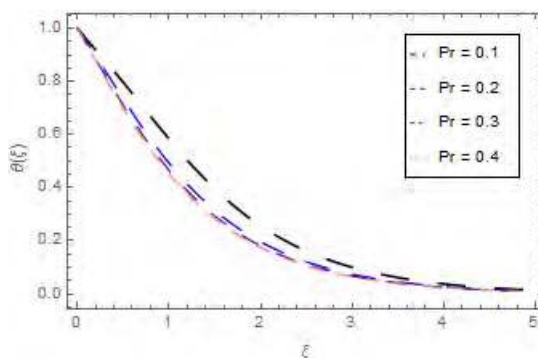


FIGURE 13. Impression of Pr on $\theta(\xi)$.

with the following properties:

$$\begin{aligned}
 L_f (y_1 + y_2 e^{-\xi} + y_3 e^{\xi}) &= 0, & L_g (y_4 + y_5 e^{-\xi} + y_6 e^{\xi}) &= 0, \\
 L_\theta (y_7 e^{-\xi} + y_8 e^{\xi}) &= 0, & L_\Phi (y_9 e^{-\xi} + y_{10} e^{\xi}) &= 0,
 \end{aligned}
 \tag{21}$$

where $y_i (i = 1 - 10)$ are constants for the general solution of the problem.

IV. HAM CONVERGENCE

The convergence of velocities fields, temperature field, and concentration field are calculated by the assisting parameters

$\tilde{h}_f, \tilde{h}_g, \tilde{h}_\theta$ and \tilde{h}_Φ of HAM are accessible in Figures 2-3. The convergence graphs are obtained at 10th order approximation. These legal regions show the convergence of HAM.

V. RESULTS AND DISCUSSION

This segment operates with the impact of dimensionless parameters arise during studying the fluid flow phenomena. These parameters include the Hartmann number (M), Hall parameter (m), ratio of rates parameter (α), couple stress parameter (K), thermal relaxation time (Ω), Prandtl number (Pr), temperature exponent (A), Brownian motion parameter (Nb), Schmidt number (Sc), and thermophoresis

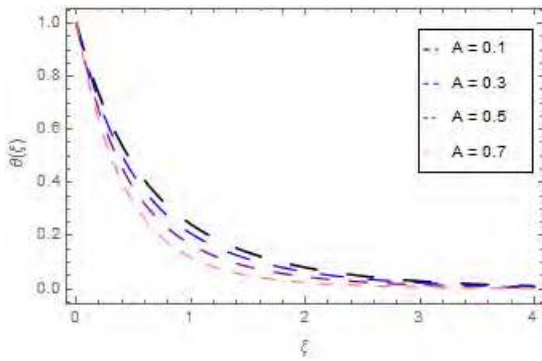


FIGURE 14. Impression of A on $\theta(\xi)$.

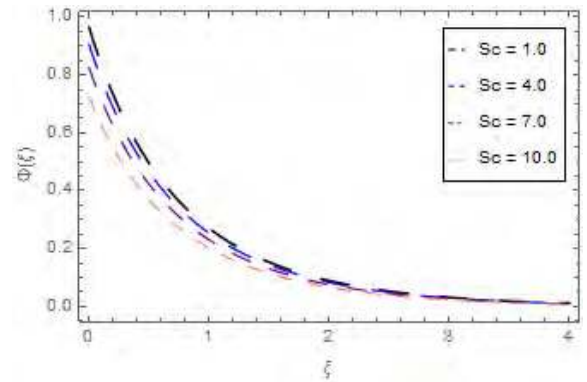


FIGURE 17. Impression of Sc on $\Phi(\xi)$.

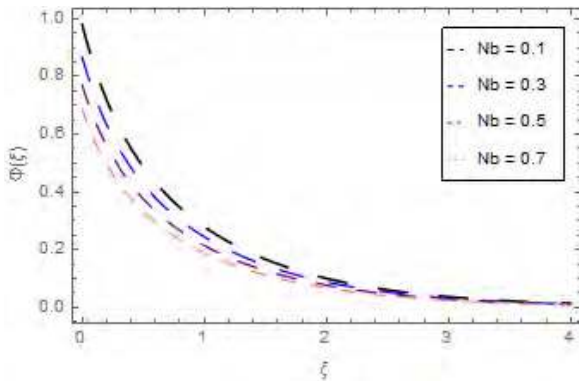


FIGURE 15. Impression of Nb on $\Phi(\xi)$.

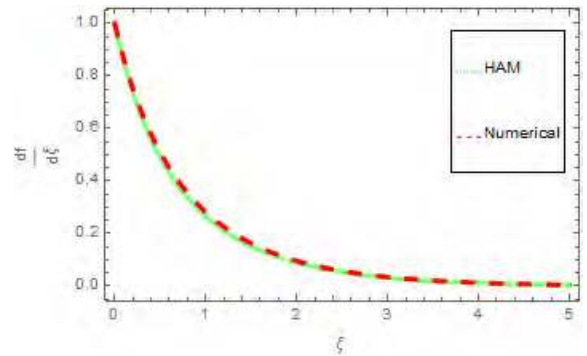


FIGURE 18. The comparison of HAM and Numerical for $\frac{df}{d\xi}$.

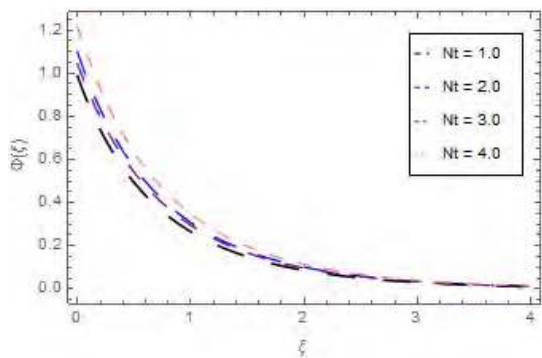


FIGURE 16. Impression of Nt on $\Phi(\xi)$.

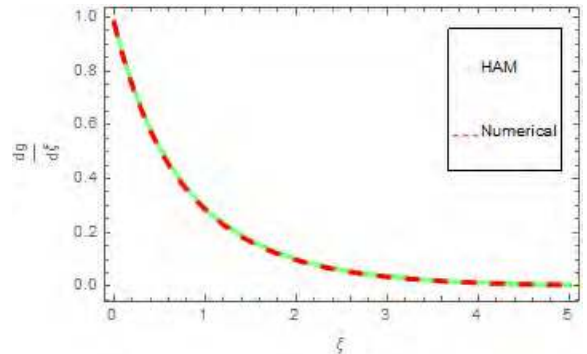


FIGURE 19. The comparison of HAM and Numerical for $\frac{dg}{d\xi}$.

parameter (Nt). The effect of M on $\frac{df}{d\xi}$ and $\frac{dg}{d\xi}$ is revealed in Figures 4-5. The Lorentz force theory says that the escalating M declines $\frac{df}{d\xi}$ and $\frac{dg}{d\xi}$. The more augmented Hartmann number M results, the more collision of molecules occurs which produce the opposing force to the flow of fluid and consequently the fluid flow velocity reduces. The effect of m on $\frac{df}{d\xi}$ and $\frac{dg}{d\xi}$ is depicted in Figures 6-7. It is clear from the figures that the escalating Hall current parameter m reduces the velocity in x -direction $\frac{df}{d\xi}$ while increases the velocity in y -direction $\frac{dg}{d\xi}$. This impact is due to the fact that the augmented Hall parameter overpowers the opposed magnetic field and speed-up the velocity of the fluid. The impression

of ratio of rates parameter α on $\frac{df}{d\xi}$ and $\frac{dg}{d\xi}$ is displayed in Figures 8-9. The augmented values of α upsurges $\frac{df}{d\xi}$ while declines $\frac{dg}{d\xi}$. This effect is because of the more dominance of α along y -direction of the fluid flow in comparison of α along x -direction of the fluid flow. The effect of couple stress parameter K on $\frac{df}{d\xi}$ and $\frac{dg}{d\xi}$ is depicted in Figure 10-11. There is a direct relationship between K and couple stress viscosity parameter n . The larger values of K indicate the more viscosity of the fluid, which delays the fluid motion and as a result the decline in $\frac{df}{d\xi}$ and $\frac{dg}{d\xi}$ is perceived. The impact of Ω on $\theta(\xi)$ is illustrated in Figure 12. It is perceived that there is an inverse relationship between Ω and $\theta(\xi)$. The growing values

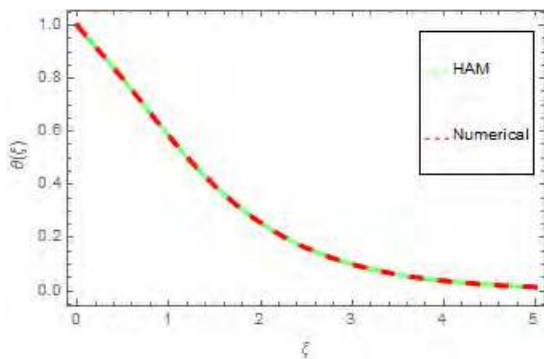


FIGURE 20. The comparison of HAM and Numerical for $\theta(\xi)$.

TABLE 1. Estimate of $C_f Re_x^{1/2}$ for α, K, M and m .

α	K	M	m	Ramzan et al. [33]	Present Study
0.1				1.43588	1.435879
0.2				1.45336	1.453365
0.3				1.51480	1.514800
0.1	0.02			1.48241	1.482409
	0.03			1.58900	1.589001
	0.01	0.1		1.37723	1.377230
		0.2		1.38939	1.389389
		0.3		1.40891	1.408910
		0.1	0.1	-----	1.153080
			0.5	-----	1.152630
			1.0	-----	1.152390

of Ω reduces the fluid flow temperature. In addition, the zero thermal relaxation time narrates to traditional Fourier’s law, so this can be deduced that the temperature is smaller than the classical Fourier’s model. The impression of Prandtl number Pr on $\theta(\xi)$ is portrayed in Figure 13. The augmented Prandtl number Pr declines $\theta(\xi)$. This effect is owing to the datum that small Pr causes large thermal conductivity but this impact is quite opposite for higher Pr . The impact of temperature exponent A on $\theta(\xi)$ is presented in Figure 14. The temperature exponent A and $\theta(\xi)$ has inverse impact. The escalating A reduces $\theta(\xi)$. The impression of Nb on $\phi(\xi)$ is portrayed in Figure 15. The escalating Nb escalates the motion of nanoparticles of the fluid, which fallouts the reduction in concentration of the fluid. Therefore, the augmented Nb reduces $\phi(\xi)$. The impact of Nt on $\phi(\xi)$ is presented in Figure 16. The augmented Nt upsurges the $\phi(\xi)$. This is due to the fact that the augmented Nt thrust the nanoparticles

TABLE 2. Estimate of $C_g Re_x^{1/2}$ for α, K, M and m .

α	K	M	m	Ramzan et al. [33]	Present Study
0.1				0.143578	0.143577
0.2				0.299583	0.299582
0.3				0.467421	0.467420
0.4				0.646402	0.646401
0.1	0.02			0.147835	0.147834
	0.03			0.154193	0.154192
	0.04			0.164693	0.164692
	0.01	0.5		0.146938	0.146937
		0.6		0.150971	0.150970
		0.7		0.155608	0.155607
			0.1	-----	0.116635
			0.5	-----	0.116349
			1.0	-----	0.115907

TABLE 3. Estimate of $Nu_x Re_x^{1/2}$ for γ, Pr, A and Ω .

γ	Pr	A	Ω	$Nu_x Re_x^{1/2}$
0.2	1.0	0.2	1.0	0.147457
0.5				0.304647
0.7				0.378621
0.9	1.2			0.438308
	1.3			0.438804
	1.4			0.439230
	1.5	0.3		0.434810
		0.4		0.429817
		0.5		0.424262
		0.6	1.1	0.423045
			1.2	0.427059
			1.3	0.430449

of the fluid flow from the warm surface and as a result the $\phi(\xi)$ upsurges. The impression of Sc on $\phi(\xi)$ is portrayed in Figure 17. Physically, the weak mass diffusivity is observed for escalating values of Sc . This weak mass diffusivity has

TABLE 4. Estimate of $Sh_x Re_x^{1/2}$ for Sc, Nb, A and Nt .

Sc	Nb	A	Nt	$Sh_x Re_x^{1/2}$
0.2	0.1	0.2	0.2	-0.954707
0.3				-0.959461
0.4				-0.964231
0.5	0.2			-0.484508
	0.3			-0.323005
	0.4			-0.242254
	0.5	0.3		-0.242798
		0.4		-0.243337
		0.5		-0.243870
		0.6	0.3	-0.366596
			0.4	-0.488794
			0.5	-0.610993

TABLE 5. The assessment of HAM and Numerical for $\frac{df}{d\xi}$.

ξ	HAM Solution	ND-Solve Solution	Absolute Error
0.0	0.999999	1.000000	0.000001
0.5	0.489683	0.489634	0.000049
1.0	0.265804	0.265763	0.000041
1.5	0.151952	0.151956	0.000004
2.0	0.089194	0.089177	0.000017
2.5	0.053097	0.053086	0.000011
3.0	0.031856	0.031849	0.000007
3.5	0.019197	0.019193	0.000004
4.0	0.011598	0.011596	0.000002
4.5	0.007018	0.007017	0.000001
5.0	0.004251	0.004250	0.000001

emotional impact on the fluid concentration and as a result the decrease in $\phi(\xi)$ is observed.

Figures 18-20 display the comparison of HAM and numerical method for velocities and temperature functions.

TABLE 6. The assessment of HAM and Numerical for $\frac{dg}{d\xi}$.

ξ	HAM Solution	ND-Solve Solution	Absolute Error
0.0	1.000000	1.000000	0.000000
0.5	0.474301	0.474055	0.000246
1.0	0.252565	0.252358	0.000207
1.5	0.142739	0.142598	0.000141
2.0	0.083208	0.083118	0.000090
2.5	0.049326	0.049269	0.000057
3.0	0.029517	0.029483	0.000034
3.5	0.017760	0.017739	0.000021
4.0	0.010720	0.010707	0.000013
4.5	0.006483	0.006475	0.000008
5.0	0.003925	0.003920	0.000005

TABLE 7. The assessment of HAM and Numerical for $\theta(\xi)$.

ξ	HAM Solution	ND-Solve Solution	Absolute Error
0.0	1.000000	1.000000	0.000000
0.5	0.710857	0.710429	0.000428
1.0	0.463897	0.463492	0.000405
1.5	0.291201	0.290912	0.000289
2.0	0.179598	0.179409	0.000189
2.5	0.109861	0.109742	0.000119
3.0	0.066936	0.066862	0.000074
3.5	0.040700	0.040655	0.000045
4.0	0.024721	0.024694	0.000027
4.5	0.015006	0.014990	0.000016
5.0	0.009106	0.009096	0.000001

VI. TABLES DISCUSSION

Tables 1 and 2 demonstrate the repercussions of incipient parameters on coefficients of skin friction in x - and y -directions respectively. These parameters are ratio of

rates (α), couple stress (K), Hartmann number (M), and Hall parameter (m). It is observed that augmented ratio of rates (α), couple stress (K) and Hartmann number (M) augmented the skin friction coefficients while the augmented Hall parameter (m) falloff the skin friction coefficients. Table 3 demonstrates the repercussions of incipient parameters on local Nusselt number. From the tabulated values, it is observed that the escalating temperature exponent, Prandtl number, and thermal relaxation time increases the local Nusselt number while reduces with the escalation in Biot number. Table 4 demonstrates the repercussions of incipient parameters on Sherwood number. It is concluded that the rising in Schmidt number, temperature exponent, and thermophoresis parameter reduce the Sherwood number while the rising Brownian motion parameter increases the Sherwood number.

Tables 5-7 display the comparison of HAM and numerical method for velocities and temperature functions.

VII. CONCLUSION

In this research work, we presented the three-dimensional flow of couple stress nanofluid with Hall current, viscous dissipation and joule heating impacts past an exponentially stretching sheet. The Cattaneo-Christov heat flux model is implemented to examine the thermal relaxation properties. The modeled equations have been transformed to nonlinear ordinary differential equations with the help of correspondence transformations. The homotopy analysis method is used to solve the proposed model.

The concluding observations are given as:

- 1) The rise in Hall parameter, Hartmann number, ratio of rates parameter, and couple stress parameter dropped the $\frac{df}{d\xi}$.
- 2) The rise in Hall parameter, Hartmann number, and ratio of rates parameter improved the $\frac{dg}{d\xi}$.
- 3) The escalation in couple stress parameter dropped the $\frac{dg}{d\xi}$.
- 4) The upsurge in thermal relaxation parameter, Prandtl number, and temperature exponent reduced the θ (ξ).
- 5) The escalation in thermophoresis parameter increased the Φ (ξ).
- 6) The upsurge in Brownian motion parameter and Schmidt number reduced the Φ (ξ).
- 7) The rise in temperature exponent, Prandtl number, and thermal relaxation time increased the Nu_x while the rise in Biot reduced the Nu_x .
- 8) The rise in Schmidt number, temperature exponent, and thermophoresis parameter reduced the Sh_x while the rise in Brownian motion parameter increased the Sh_x .

CONFLICTS OF INTEREST

The author declares that they have no competing interests.

ACKNOWLEDGMENT

This project was supported by the Theoretical and Computational Science (TaCS) Center under Computational and

Applied Science for Smart Innovation Research Cluster (CLASSIC), Faculty of Science, KMUTT.

REFERENCES

- [1] S. U. S. Choi and J. A. Eastman, "Enhancing thermal conductivity of fluids with nanoparticles," *ASME-Publications-Fed*, vol. 231, pp. 99–106, Jan. 1995.
- [2] X. Q. Wang and A. S. Mujumdar, "Heat transfer characteristics of nanofluids: A review," *Int. J. Therm. Sci.*, vol. 46, no. 1, pp. 1–19, 2007.
- [3] J. A. Eastman, S. R. Phillpot, S. U. S. Choi, and P. Keblinski, "Thermal transport in nanofluids," *Annu. Rev. Mater. Res.*, vol. 34, pp. 219–246, Aug. 2004.
- [4] J. A. Eastman, S. U. S. Choi, S. Li, W. Yu, and L. J. Thompson, "Anomalous increased effective thermal conductivities of ethylene glycol-based nanofluids containing copper nanoparticles," *Appl. Phys. Lett.*, vol. 78, no. 6, pp. 718–720, 2001.
- [5] S. M. S. Murshed, K. C. Leong, and C. Yang, "Enhanced thermal conductivity of TiO₂—Water based nanofluids," *Int. J. Therm. Sci.*, vol. 44, no. 4, pp. 367–373, 2005.
- [6] S. El B. Maïga, C. T. Nguyen, N. Galanis, and G. Roy, "Heat transfer behaviours of nanofluids in a uniformly heated tube," *Superlattice. Microst.*, vol. 35, nos. 3–6, pp. 543–557, 2004.
- [7] V. Bianco, F. Chiacchio, O. Manca, and S. Nardini, "Numerical investigation of nanofluids forced convection in circular tubes," *Appl. Therm. Eng.*, vol. 29, nos. 17–18, pp. 3632–3642, 2009.
- [8] R. K. Tiwari and M. K. Das, "Heat transfer augmentation in a two-sided lid-driven differentially heated square cavity utilizing nanofluids," *Int. J. Heat Mass Tran.*, vol. 50, nos. 9–10, pp. 2002–2018, May 2007.
- [9] J. Buongiorno, "Convective transport in nanofluids," *J. Heat Transf.*, vol. 128, no. 3, pp. 240–250, 2006.
- [10] A. Kasaeian, "Nanofluid flow and heat transfer in porous media: A review of the latest developments," *Int. J. Heat Mass Trans.*, vol. 107, pp. 778–791, Apr. 2017.
- [11] S. Mota and S. Shateyi, "The effects of chemical reaction, Hall, and ion-slip currents on MHD micropolar fluid flow with thermal diffusivity using a novel numerical technique," *J. App. Math.*, vol. 9, pp. 1–30, Nov. 2012.
- [12] T. Hayat, H. Zahir, A. Alsaedi, and B. Ahmad, "Hall current and Joule heating effects on peristaltic flow of viscous fluid in a rotating channel with convective boundary conditions," *Results Phys.*, vol. 7, pp. 2831–2836, Jan. 2017.
- [13] T. Hayat and M. Nawaz, "Hall and ion-slip effects on three-dimensional flow of a second grade fluid," *Int. J. Numer. Method Fluids*, vol. 66, no. 2, pp. 183–193, 2011.
- [14] T. Hayat, A. Bibi, H. Yasmin, and B. Ahmad, "Simultaneous effects of Hall current and homogeneous/heterogeneous reactions on peristalsis," *J. Taiwan Inst. Chem. Eng.*, vol. 58, pp. 28–38, Jan. 2016.
- [15] T. Hayat, M. Awais, M. Nawaz, S. Iram, and A. Al Saedi, "Mixed convection three-dimensional flow with Hall and ion-slip effects," *Int. J. Nonlinear Sci. Number Simul.*, vol. 14, nos. 3–4, pp. 167–177, 2013.
- [16] T. Hayat and M. Nawaz, "Soret and Dufour effects on the mixed convection flow of a second grade fluid subject to Hall and ion-slip currents," *Int. J. Number Method's Fluids*, vol. 66, no. 9, pp. 1073–1099, 2011.
- [17] T. Hayat, M. Shafique, A. Tanveer, and A. Alsaedi, "Hall and ion slip effects on peristaltic flow of Jeffrey nanofluid with joule heating," *J. Magn., Magn. Mater.*, vol. 407, pp. 51–59, Jun. 2016.
- [18] M. Nawaz, T. Hayat, and A. Alsaedi, "Mixed convection three-dimensional flow in the presence of Hall and ion-slip effects," *J. Heat Trans.*, vol. 135, no. 4, p. 042502, May 2013.
- [19] M. Nawaz, S. Rana, I. H. Qureshi, and T. Hayat, "Three-dimensional heat transfer in the mixture of nanoparticles and micropolar MHD plasma with Hall and ion slip effects," *AIP Adv.*, vol. 8, no. 10, p. 105109, 2018.
- [20] T. Hayat, M. Iqbal, H. Yasmin, and F. Alsaadi, "Hall effects on peristaltic flow of couple stress fluid in an inclined asymmetric channel," *Int. J. Biomathemat.*, vol. 7, no. 5, p. 1450057, 2014.
- [21] M. Ramzan, J. D. Chung, and N. Ullah, "Radiative magnetohydrodynamic nanofluid flow due to gyrotactic microorganisms with chemical reaction and non-linear thermal radiation," *Int. J. Mech. Sci.*, vol. 130, pp. 31–40, Sep. 2017.

- [22] M. Sheikholeslami and S. A. Shehzad, "Magneto-hydrodynamic nanofluid convective flow in a porous enclosure by means of LBM," *Int. J. Heat Mass Trans.*, vol. 113, pp. 796–805, Oct. 2017.
- [23] P. Besthapu, R. U. Haq, S. Bandari, and Q. M. Al-Mdallal, "Mixed convection flow of thermally stratified MHD nanofluid over an exponentially stretching surface with viscous dissipation effect," *J. Taiwan Inst. Chem. E.*, vol. 71, pp. 307–314, Feb. 2017.
- [24] A. Dawar, Z. Shah, M. Idress, W. Khan, S. Islam, and T. Gul, "Impact of thermal radiation and heat source/sink on Eyring–Powell fluid flow over an unsteady oscillatory porous stretching surface," *Math. Comput. Appl.*, vol. 23, no. 2, p. 20, 2018. doi: [10.3390/mca23020020](https://doi.org/10.3390/mca23020020).
- [25] S. O. Alharbi et al., "Entropy generation in MHD Eyring–Powell fluid flow over an unsteady oscillatory porous stretching surface under the impact of thermal radiation and heat source/sink," *Appl. Sci.*, vol. 8, p. 2588, Dec. 2018.
- [26] Z. Shah, A. Dawar, S. Islam, I. Khan, and D. L. C. Ching, "Darcy–Forchheimer flow of radiative carbon nanotubes with microstructure and inertial characteristics in the rotating frame," *Stud. Thermal Eng.*, vol. 2, pp. 823–832, Sep. 2018.
- [27] A. Khan et al., "Darcy–Forchheimer flow of MHD CNTs nanofluid radiative thermal behaviour and convective non uniform heat source/sink in the rotating frame with microstructure and inertial characteristics," *AIP Adv.*, vol. 8, no. 12, p. 125024, 2018. doi: [10.1063/1.5066223](https://doi.org/10.1063/1.5066223).
- [28] A. S. Khan, Y. Nie, Z. Shah, A. Dawar, W. Khan, and S. Islam, "Three-dimensional nanofluid flow with heat and mass transfer analysis over a linear stretching surface with convective boundary conditions," *Appl. Sci.*, vol. 8, no. 11, p. 2244, 2018.
- [29] Z. Shah, W. Khan, A. Dawar, and I. Muhammad, "Unsteady squeezing flow of magneto-hydrodynamic carbon nanotube nanofluid in rotating channels with entropy generation and viscous dissipation," *Adv. Mech. Eng.*, vol. 11, no. 1, pp. 1–18, 2019.
- [30] M. Sheikholeslami and D. D. Ganji, "Numerical investigation of nanofluid free convection under the influence of electric field in a porous enclosure," *J. Mol. Liquids*, vol. 249, no. 3, pp. 1212–1221, 2018.
- [31] M. Sheikholeslami, "CuO-water nanofluid flow due to magnetic field inside a porous media considering Brownian motion," *J. Mol. Liquids*, vol. 249, pp. 921–929, Jan. 2018.
- [32] A. Dawar, Z. Shah, W. Khan, S. Islam, and M. Idrees, "An optimal analysis for Darcy–Forchheimer 3-D Williamson nanofluid flow over a stretching surface with convective conditions," *Adv. Mech. Eng.*, vol. 11, no. 3, pp. 1–15, 2019. doi: [10.1177/1687814019833510](https://doi.org/10.1177/1687814019833510).
- [33] M. Ramzan, M. Sheikholeslami, M. Saeed, and J. D. Chung, "On the convective heat and zero nanoparticle mass flux conditions in the flow of 3D MHD Couple Stress nanofluid over an exponentially stretched surface," *Sci. Rep.*, vol. 9, p. 562, Jan. 2019.
- [34] J. B. J. Fourier, *Théorie Analytique de la Chaleur*. Chez Firmin Didot, père et fils, Paris, France, 1822.
- [35] C. Cattaneo, "Sulla conduzione del calore," in *Some Aspects of Diffusion Theory* (C.I.M.E. Summer Schools), vol. 42, A. Pignedoli, Eds. Berlin, Germany: Springer, 2011, pp. 485–485. doi: [10.1007/978-3-642-11051-1_5](https://doi.org/10.1007/978-3-642-11051-1_5).
- [36] C. I. Christov, "On frame indifferent formulation of the Maxwell–Cattaneo model of finite-speed heat conduction," *Mech. Res. Commun.*, vol. 36, no. 4, pp. 481–486, 2009.
- [37] B. Straughan, *Stability and Wave Motion in Porous Media*, vol. 165. New York, NY, USA: Springer, 2008, pp. 14–437.
- [38] B. Straughan, "Thermal convection with the Cattaneo–Christov model," *Int. J. Heat Mass Transfer*, vol. 53, no. 1, pp. 95–98, 2010.
- [39] S. Han, L. Zheng, C. Li, and X. Zhang, "Coupled flow and heat transfer in viscoelastic fluid with Cattaneo–Christov heat flux model," *Appl. Math. Lett.*, vol. 38, pp. 87–93, Dec. 2014.
- [40] J. A. Khan, M. Mustafa, T. Hayat, and A. Alsaedi, "Numerical study of Cattaneo–Christov heat flux model for viscoelastic flow due to an exponentially stretching surface," *PLoS ONE*, vol. 10, no. 9, p. e0137363, 2015.
- [41] T. Hayat and S. Nadeem, "Flow of 3D Eyring–Powell fluid by utilizing Cattaneo–Christov heat flux model and chemical processes over an exponentially stretching surface," *Results Phys.*, vol. 8, pp. 397–403, May 2018.
- [42] V. Tibullo and V. Zampoli, "A uniqueness result for the Cattaneo–Christov heat conduction model applied to incompressible fluids," *Mech. Res. Commun.*, vol. 38, no. 1, pp. 9–77, 2011.
- [43] M. Ciarletta and B. Straughan, "Uniqueness and structural stability for the Cattaneo–Christov equations," *Mech. Res. Commun.*, vol. 37, no. 5, pp. 445–447, 2010.
- [44] S. A. M. Haddad, "Thermal instability in Brinkman porous media with Cattaneo–Christov heat flux," *Int. J. Heat Mass Transfer*, vol. 68, pp. 659–668, Jan. 2014.
- [45] M. Mustafa, "Cattaneo–Christov heat flux model for rotating flow and heat transfer of upper-convected Maxwell fluid," *AIP Adv.*, vol. 5, no. 4, p. 047109, 2015.
- [46] T. Hayat, M. Farooq, A. Alsaedi, and F. Al-Solamy, "Impact of Cattaneo–Christov heat flux in the flow over a stretching sheet with variable thickness," *AIP Adv.*, vol. 5, no. 8, p. 087159, 2015.
- [47] M. Waqas, T. Hayat, M. Farooq, S. A. Shehzad, and A. Alsaedi, "Cattaneo–Christov heat flux model for flow of variable thermal conductivity generalized Burgers fluid," *J. Mol. Liquids*, vol. 220, pp. 642–648, Aug. 2016.
- [48] J. Li, L. Zheng, and L. Liu, "MHD viscoelastic flow and heat transfer over a vertical stretching sheet with Cattaneo–Christov heat flux effects," *J. Mol. Liquids*, vol. 221, pp. 19–25, Sep. 2016.
- [49] Z. Shah, A. Dawar, I. Khan, S. Islam, D. L. C. Ching, and A. Z. Khan, "Cattaneo–Christov model for electrical magnetite micropolar Casson ferrofluid over a stretching/shrinking sheet using effective thermal conductivity model," *Case Stud. Thermal Eng.*, vol. 13, p. 100352, Mar. 2019.
- [50] M. Muskat, *The Flow of Homogeneous Fluids Through Porous Media*. Ann Arbor, MI, USA: Edwards, 1946.
- [51] M. A. Seddeek, "Influence of viscous dissipation and thermophoresis on Darcy–Forchheimer mixed convection in a fluid saturated porous media," *J. Colloid Interface Sci.*, vol. 293, pp. 137–142, 2006. doi: [10.1016/j.jcis.2005.06.039](https://doi.org/10.1016/j.jcis.2005.06.039).
- [52] D. Pal and H. Mondal, "Hydromagnetic convective diffusion of species in Darcy–Forchheimer porous medium with non-uniform heat source/sink and variable viscosity," *Int. Commun. Heat Mass Transfer*, vol. 39, no. 7, pp. 913–917, 2012.
- [53] M. A. Sadiq and T. Hayat, "Darcy–Forchheimer flow of magneto Maxwell liquid bounded by convectively heated sheet," *Results Phys.*, vol. 6, pp. 884–890, 2016.
- [54] T. Gul, "Scattering of a thin layer over a nonlinear radially extending surface with magneto-hydrodynamic and thermal dissipation," *Surf. Rev. Lett.*, vol. 26, no. 1, p. 1850123, 2019.
- [55] T. Gul, M. A. Khan, A. Khan, and M. Shuaib, "Fractional-order three-dimensional thin-film nanofluid flow on an inclined rotating disk," *Eur. Phys. J. Plus*, vol. 133, p. 500, Dec. 2018.
- [56] L. Ali, S. Islam, T. Gul, A. S. Alshomrani, I. Khan, and A. Khan, "Magneto-hydrodynamics thin film fluid flow under the effect of thermophoresis and variable fluid properties," *AICHE J.*, vol. 63, no. 11, pp. 5149–5158, 2017. doi: [10.1002/aic.15794](https://doi.org/10.1002/aic.15794).
- [57] T. G. Gohar, K. Waris, S. Muhammad, A. K. Muhammad, and B. Ebenezer, "MWCNTs/SWCNTs nanofluid thin film flow over a nonlinear extending disc: OHAM solution," *J. Therm. Sci.*, vol. 28, no. 1, pp. 115–122, 2019.
- [58] T. Gul et al., "The study of the entropy generation in a thin film flow with variable fluid properties past over a stretching sheet," *Adv. Mech. Eng.*, vol. 10, no. 11, pp. 1–15, 2018.
- [59] N. S. Khan et al., "Thermophoresis and thermal radiation with heat and mass transfer in a magneto-hydrodynamic thin-film second-grade fluid of variable properties past a stretching sheet," *Eur. Phys. J. Plus*, vol. 132, p. 11, Jan. 2017.
- [60] B. J. Gireeshn, K. Ganesh Kumar, M. R. Krishnamurthy, S. Manjunatha, and N. G. Rudraswamy, "Impact of ohmic heating on MHD mixed convection flow of Casson fluid by considering cross diffusion effect," *Nonlinear Eng.*, vol. 8, no. 1, pp. 380–388, 2018.
- [61] K. Ganesh Kumar, G. K. Ramesh, and B. J. Gireesha, "Thermal analysis of generalized burgers nanofluid over a stretching sheet with nonlinear radiation and non-uniform heat source/sink," *Arch. Thermodyn.*, vol. 39, no. 2, pp. 97–122, 2018.
- [62] B. J. Gireeshn, K. G. Kumar, and S. Manjunatha, "Impact of chemical reaction on MHD 3D flow of a nanofluid containing gyrotactic microorganism in the presence of uniform heat source/sink," *Int. J. Chem. Reactor Eng.*, vol. 16, no. 12, 2018.
- [63] K. K. Ganesh and A. J. Chamkha, "Forchheimer flow and heat transfer of water-based Cu nanoparticles in convergent/divergent channel subjected to particle shape effect," *Eur. Phys. J. Plus*, vol. 134, p. 107, Mar. 2019.

- [64] B. J. Gireesha et al., "Enhancement of heat transfer in an unsteady rotating flow for the aqueous suspensions of single wall nanotubes under nonlinear thermal radiation: A numerical study," *Colloid Polym. Sci.*, vol. 296, no. 9, pp. 1501–1508, Sep. 2018.
- [65] B. J. Gireesha, G. Kumar, G. K. Ramesh, and B. C. Prasannakumara, "Nonlinear convective heat and mass transfer of Oldroyd-B nanofluid over a stretching sheet in the presence of uniform heat source/sink," *Results Phys.*, vol. 9, pp. 1555–1563, Jun. 2018.
- [66] M. G. Reddy, M. V. V. N. L. S. Rani, K. G. Kumar, and B. C. Prasannakumara, "Cattaneo-Christov heat flux and non-uniform heat-source/sink impacts on radiative Oldroyd-B two-phase flow across a cone/wedge," *J. Braz. Soc. Mech. Sci. Eng.*, vol. 40, p. 95, Feb. 2018.
- [67] B. J. Gireesha, K. G. Kumar, N. G. Rudraswamy, and S. Manjunatha, "Effect of viscous dissipation on three dimensional flow of a nanofluid by considering a gyrotactic microorganism in the presence of convective condition," *Defect Diffusion Forum*, vol. 388, pp. 114–123, Oct. 2018.
- [68] P. Kumam, Z. Shah, A. Dawar, H. U. Rasheed, and S. Islam, "Entropy generation in MHD radiative flow of CNTs Casson nanofluid in rotating channels with heat source/sink," *Math. Problems Eng.*, vol. 2019, Art. no. 9158093, Jun. 2019.
- [69] T. Hayat, S. Qayyum, M. Imtiaz, and A. Alsaedi, "Influence of Cattaneo-Christov heat flux on MHD Jeffrey, Maxwell, and oldroyd-B nanofluids with homogeneous-heterogeneous reaction," *Symmetry*, vol. 11, no. 3, p. 439, 2019.



EBRAHEEM O. ALZHRANI received the Ph.D. degree from Dundee University, U.K. He is currently an Associate Professor with King Abdulaziz University, Jeddah, Saudi Arabia. He has written several papers in various fields of applied mathematics. His research interests include mechanics, applied analysis, mathematical biology, and mathematical ecology.



POOM KUMAM received the Ph.D. degree in mathematics from Naresuan University, Thailand. He is currently a Full Professor with the Department of Mathematics, King Mongkut's University of Technology Thonburi (KMUTT), where he is also the Head of KMUTT Fixed Point Theory and Applications Research Group and the Theoretical and Computational Science Center (TaCS-Center) and also the Director of the Computational and Applied Science for Smart Innovation Cluster (CLASSIC Research Cluster). He has authored or coauthored more than 400 international peer reviewed journals. His current research interests include fixed point theory and applications, computational fixed point algorithms, nonlinear optimization and control theory, and optimization algorithms.



ZAHIR SHAH received the M.Sc. Degree from the University of Malaknad lower Dir chak-dara, Khyber Pakhtunkhwa, Pakistan, the M.Phil. degree from Islamia College University, Peshawar, Pakistan, and the Ph.D. degree from Abdul Wali Khan University Mardan Pakistan. He is currently an Assistant Professor with the Ghandhara University of Science & Technology, Peshawar. He has written several papers and books in various filed of mechanical engineering. His research interests are nanofluid, CFD, simulation, heat transfer, MHD, Hall effect, mesoscopic modeling, nonlinear science, magnetohydrodynamic, ferrohydrodynamic, electrohydrodynamic, and heat exchangers.



ABDUL JABBAR KHAN received the M.Sc. degree in electrical engineering from the University of Engineering and Technology at Peshawar, Peshawar, Pakistan. He was with engineering university and affiliated institutes as the Trainee, a Lab Engineer, Labs in Charge, and a Lecturer for more than six years. His research articles include Verification of Short Circuit Test Results of Salient Poles Synchronous Generator and Design of Vehicle Health and Position Telemetry System for Management. His research interest includes mathematical modeling of electrical machines using FEM analysis and Park's transformation.



ABDULLAH DAWAR received the bachelor's degree in mathematics from Islamia College University, Peshawar, Pakistan. He is currently pursuing the M.Sc. degree in mathematics with the Qurtuba University of Science and Information Technology. He is also a Researcher with the Zahir Shah's lab. He has published several articles in various Journals. His research interests include magnetohydrodynamic, nanofluid, heat transfer, Hall effect, electrohydrodynamic, and heat exchangers.



SAEED ISLAM received the M.Sc. degree from Quaid-e-Azam University, Islamabad, Pakistan, and the Ph.D. degree from the Harbin Institute of Technology Shenzhen Graduate School, China. He is currently a Professor/Chairman with the Department of Mathematics, Abdul Wali Khan University, Mardan, Pakistan. He has written several papers and books in various filed of mechanical engineering. His research interests include nanofluid, CFD, simulation, heat transfer, MHD, Bio mathematics, mesoscopic modeling, nonlinear science, magnetohydrodynamic, ferrohydrodynamic, electrohydrodynamic, and heat exchangers.

...